A Reliable Control for the Ammonia Loop Facing Limit-Cycle and *Snowball* Effects

Maurizio Rovaglio, Davide Manca, and Francesco Cortese
Dipartimento di Chimica, Materiali ed Ingegneria Chimica "G. Natta" Politecnico di Milano, P.zza Leonardo da Vinci 32, 20133 Milano, Italy

DOI 10.1002/aic.10103
Published online in Wiley InterScience (www.interscience.wiley.com).

Autothermal catalytic reactors may show limit cycle behavior because of the simultaneous presence of inverse response and thermal feedback actions. In this study, a classical ammonia reactor (two beds, radial flow) was considered, and simulated together with the overall synthesis loop. Oscillations, caused by feed gas temperature disturbances, have been confirmed, whereas a pressure dependent hysteresis pattern appeared when the temperature is reset to the original design value. A more sensitive dynamic behavior is highlighted for the synthesis loop compared with the reactor alone, because of energy and material recycles. Finally, a control strategy extended to the overall synthesis loop has been tested in order to avoid dangerous dynamics and undesired reactor shutdown. The proposed control configuration, applied to the overall synthesis loop, is able to face and avoid both "snowball" effects and dangerous limit cycle conditions. © 2004 American Institute of Chemical Engineers *AIChE J,* 50: 1229–1241, 2004
Keywords: Ammonia, limit-cycle, bifurcation, control, dynamics

Introduction

In a recent article, Morud and Skogestad (1998) describe the occurrence of an industrial accident in an ammonia production plant. The accident was caused by a sudden loss of stability induced by a decrease of the reactor pressure. The instability determined that the steady state was moving to a new dynamic regime characterized by sustained oscillations. In Morud and Skogestad's work, the analysis was performed through a nonlinear model consisting of two partial differential equations (PDE) limited to the reactor modeling, but capable of qualitatively interpreting the accident data. The onset oscillation was correctly described despite the model simplicity, and in order to reduce the risk of instability, a control strategy has been proposed but not verified. A minor limitation of the Morud and Skogestad's approach is the lack of a complete dynamic analysis able to prevent the possibility of other multistability scenarios that might be discovered in actual operations. In a following work by Mancusi et al. (1999), the results of a complete dynamic analysis were presented. In that article, the same model proposed by Morud and Skogestad was adopted to show how to improve the model predictive capability. Reactor pressure and heat exchanger efficiency were considered as bifurcation parameters and a complete description of both static and dynamic attractors has been reported for typical operating conditions. However, the analysis was limited only to the ammonia reactor, disregarding the external heat-mass recycles that characterize the ammonia synthesis loop, and without clearly addressing the control problem and the related design.

The aim of this work is to address the design and development of a reliable control system for the overall ammonia synthesis loop. The loop structure considered here was taken from literature (Nielsen, 1995), and it is shown in Figure 1. The process examined is composed by a synthesis reactor, a cascade of heat exchangers and two separation units. As shown in Figure 1, there are three different recycles in the adopted layout. The first one is identified by the third heat exchanger, where the effluent stream from the reactor releases heat to the stream that is feeding the reactor. This configuration is typical of an autothermal system where the feedstream is preheated by

Correspondence concerning this article should be addressed to M. Rovaglio at maurizio.rovaglio@polimi.it.

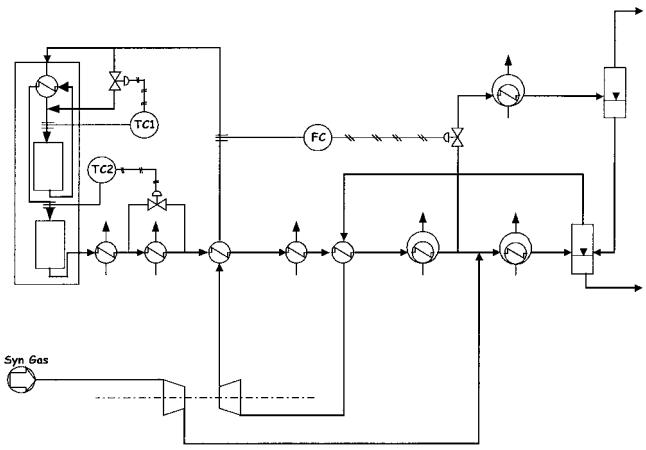

Figure 1. Layout and main control scheme for the ammonia synthesis loop.

the hot outlet stream. The second thermal recycle is represented by the fifth heat exchanger, which is also used to preheat the recycle stream to the reactor by means of the heat coming from the hot stream leaving the reactor. Finally, the flash that separates the liquid ammonia product from the unreacted gas involves a material recycle. Indeed, hydrogen conversion for each reacting-pass is approximately in a range of 30%, and it is necessary to provide a recycle of the unconverted material to the process unit.

The control system to be adopted, for the process in object, should be able to reject external disturbances on the main process variables, and to face uncertainty on the implemented control settings. For this purpose, an extended dynamic analysis has been performed to evaluate the impact of heat and material recycles addressing the multistable behavior from one side, and the controllability issue from the other. It must be underlined that a bifurcation diagram analysis is beyond the scope of this work because the subject requires specific attention, efforts and a detailed analysis for which we refer to the specific literature (Mancusi et al., 2000), or to the future development of this research. However, a detailed analysis on the most appropriate model scale description is carried out for a better and quantitative understanding of the operating conditions range where the instability can occur. Therefore, the momentum balance and the heterogeneous reactor model have been investigated as possible improvements of the previous work. Moreover, the model extension to the overall synthesis loop implies new equations related to a cascade of heat exchangers as well as two stages flash where the ammonia is condensed and separated as a liquid product, whereas the gas is recycled to the reaction stage. It is important to underline that two of the aforementioned heat exchangers are adopted for feed preheating and, thus, involving strong heat system integration. Consequently, the impact of such a double heat recycle as well as the material one, related to the unreacted gas, is analyzed in terms of both dynamic behavior and stability. Particularly, the results clearly show that, with this more complete layout, small disturbances imposed on the input parameters can generate important output variations (snowball effect). Moreover, sustained oscillations can be induced by smaller disturbances than those pointed out by previous studies. Finally, a conventional control scheme (see Figure 1) is analyzed in terms of pairing and optimal control settings. The main reactor control loops (Jennings, 1991; Nielsen, 1995) are constituted by the inlet bed temperatures, which are controlled through the heat exchanger bypass (see Figure 1). Therefore, the loop conversion and the thermal regime can be maintained and, thus, the external disturbances are rejected. With reference to such a control scheme, the sensitivity analysis here performed shows that inaccuracy on the control parameters, because of poor tuning, can lead to sustained oscillations with respect to pressure disturbances even in the presence of closed-loop conditions. Moreover, a flow rate control on the main recycle stream, whereas avoiding the "snowball" effect, can also improve the "process robustness" with respect to the rise of limit cycle conditions.

Reactor Model

The ammonia converter investigated here is a radial flow fixed-bed reactor. The pressure shell is assumed to be adiabatic and it hosts an internal-bed heat exchanger. Figure 2 shows the flow pattern where the gas enters the converter through two main inlets at the bottom of the pressure shell; then it moves upward through the annular space between the catalytic baskets and the pressure shell. From the top of the converter, the gas goes to the tube side of the internal-bed heat exchanger where it reaches the reaction temperature required by the first bed. It flows inward through the catalytic basket, and again it crosses the heat exchanger (shell side), where it cools down to the temperature required by the second catalytic basket. From one of the two bottom inlets is derived a small part of the cold

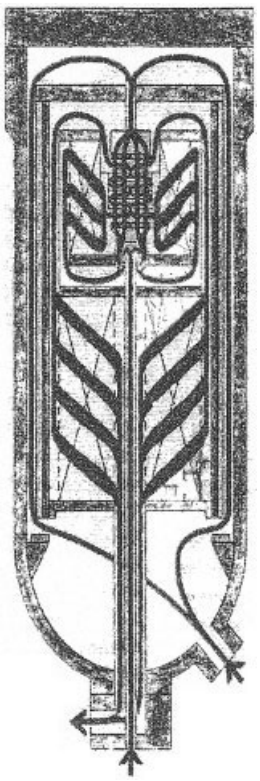

Figure 2. Flow patterns inside the ammonia converter.

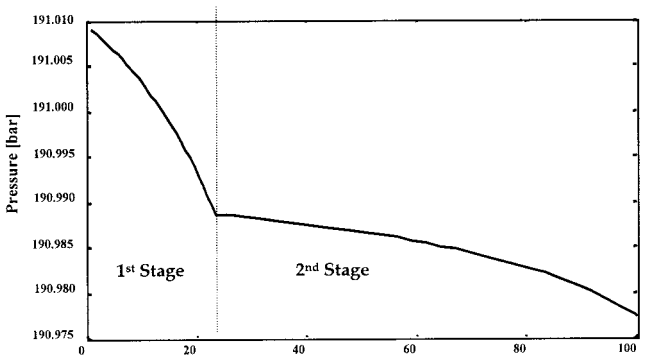

Figure 3. Pressure drops along the two catalytic beds.

syngas entering the first bed without preheating. This bypass ("cold shot") adjusts the gas temperature to the first bed.

The equations for a pseudohomogeneous model of the reactor unit include energy and mass dynamic balances, and a stationary momentum balance which describes the pressure drops along the catalytic beds. This last relationship is based on the assumption that the pressure dynamics is very fast when compared to the mass and heat transients. Consequently, it can be described, approximately, as a sequence of steady-state conditions. The derived equations are namely

$$\frac{\partial c_i}{\partial t} = -v_x \cdot \frac{\partial c_i}{\partial x} + D_{i,mix} \cdot \frac{\partial^2 c_i}{\partial x^2} + \nu_i \cdot R_{NH_3} \tag{1}$$

$$\rho_{cat} \cdot C_{p,cat} \cdot \frac{\partial T}{\partial t} = -\rho_{gas} \cdot C_{p,gas} \cdot v_x \cdot \frac{\partial T}{\partial x} + k_g \cdot \frac{\partial^2 T}{\partial x^2} + (-\Delta H_r) \cdot R_{NH_3} \tag{2}$$

$$0 = -\frac{\partial p}{\partial x} \pm \frac{G_{IN}^2}{2g\rho}\left(\frac{D_{IN}}{\psi \cdot D_S} \cdot \frac{(1-\theta_e)}{\theta_e^3}\left(\frac{100}{\mathrm{Re}_{IN}} \ln \frac{D_{OUT}}{D_{IN}} + 1.75 \cdot \left(1 - \frac{D_{IN}}{D_{OUT}}\right)\right) \pm \frac{1}{\theta_e^2}\left(1 - \left(\frac{D_{IN}}{D_{OUT}}\right)^2\right)\right) \tag{3}$$

The last equation is based on a modified Ergun expression (Jennings, 1991) where the plus sign is chosen when the flow is moving centripetally. This type of reactor gives rise to a low-pressure drop because of the large section area, and the short length of the catalyst bed where the gas is passing through. The simulation results reported in Figure 3 confirm this hypothesis and allow Eq. 3 to be neglected. The holdup term ($\delta c_i/\delta t$) for the gas phase in Eq. 1 is also negligible because of the residence time that is clearly lower than the characteristic time of the temperature response to any disturbance ($\approx$ 50 s vs. 15 min). Mancusi et al. (2000) also tested such an assumption for both stationary and periodic solutions. As far as the modeling of the catalytic reactor is concerned, it can be represented by either a continuous system or a sequence of stirred-tank reactors. The latter model, also called the mixing-cell model, has the capability of transforming a partially differential equation (PDE) system into an ordinary differential equation (ODE) system. Considering a k^{th} discretization cell

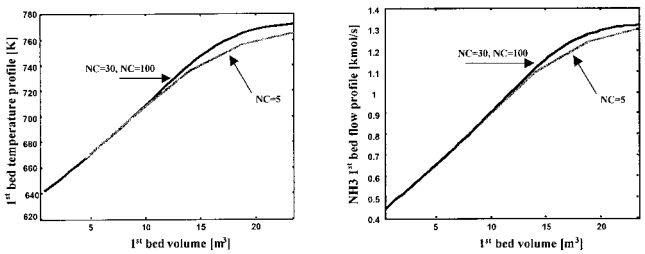

Figure 4. Temperature and NH_3-flow steady-state profiles along the bed volume.

(with k from 1 to NC) and the aforementioned assumptions, Eqs. 1 and 2 become

$$0 = F_{i,k-1} - F_{i,k} + \nu_i \cdot R_{NH_3} \cdot V_k \tag{4}$$

$$C_{p,cat} \cdot \rho_{cat} \cdot V_k \cdot \frac{dT_k}{dt} = (T_{k-1} - T_k) \cdot C_{p,mix,k-1} \cdot F_{tot,k-1} + R_{NH_3} \cdot (-\Delta H_k) \cdot V_k \tag{5}$$

The system arising from this model is constituted by algebraic and differential equations (DAEs), as already underlined, the gas-phase holdups are neglected. The main point to be emphasized is that a unique asymptotic temperature and NH_3-flow profile are obtained for steady-state conditions, (Figure 4) with a cells number NC $>$ 30. Hence, two different dynamic evolutions are derived along the transient when NC $<$ 30. In Figure 5, which refers to the dynamic evolution determined by a disturbance on the inlet temperature, two significantly different behaviors can be pointed out: the former is the reactor shutdown when NC=5 or 30, whereas the second is the limit cycle behavior with NC=100. The cells number is related to the energy and material dispersion in the gas flow direction: the fewer the cells the greater their depth, and also, the characteristic length of the dispersion phenomena. For a fully developed turbulent flow, the Reynolds number referred to the catalyst particle should be in the order of 10^2. For example, in the case examined here it becomes $\mathrm{Re}_p = (\rho \cdot v_0)/(\psi \cdot a \cdot \mu) \cong 7 \cdot 10^2$ where the characteristic length is assumed equal to the particles diameter (D_p=3 mm). However, if the molecular

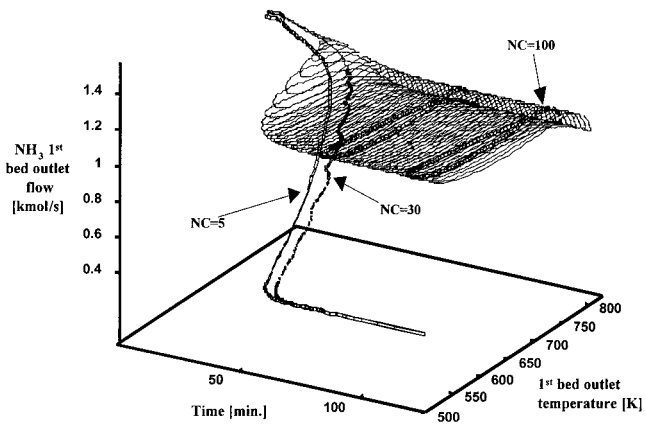

Figure 5. Dynamic evolution of the phase diagram at a pressure of 190 bar.

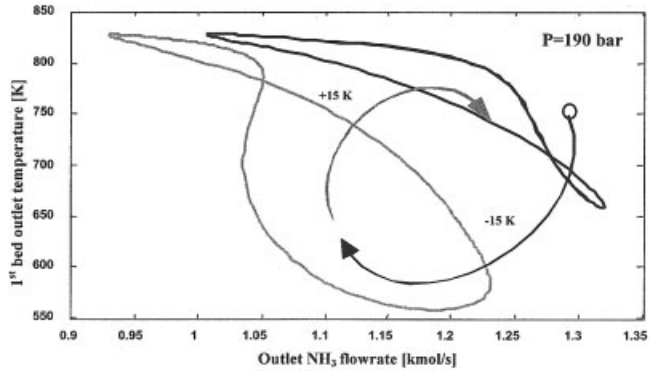

Figure 6. Hysteresis pattern related to a disturbance of ± 15 K and referring to NC=100.

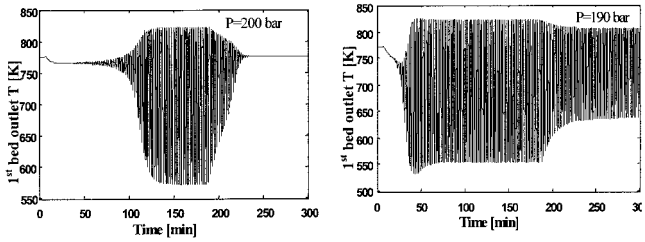

Figure 7. At the operating pressure of 200 bar, the hysteresis disappears (both diagrams refer to a disturbance of ± 15 K).

contribution to transport phenomena is negligible, the effective thermal and material diffusivities are equal because the transport mechanism is exactly the same. Such asymptotic condition is reached when Re_P is in the order of 10^2; at these values, Re_{Dp}.Pr = 2 that means $Pe_L/2$ = L/Dp = NC. Thus, Dp becomes the measure to be adopted for each cell. Therefore, to obtain each cell of such depth, about 100 cells are needed according to the geometry of the first examined catalytic basket. No significant difference in terms of dynamic evolution appears when comparing alternative simulations with NC>100. Similar conclusions may be drawn for the second basket, where about 200 cells are needed because the difference between external and internal radii is greater. Further details are briefly reported in Appendix A referring on the kinetic expression adopted to follow the reactor evolution plus the equations of the internal heat exchanger.

Performing the dynamic analysis of such a reactor model, an interesting result can be derived when considering a temperature disturbance on the inlet flow. After the disturbance, when a limit cycle is reached, if the original conditions are reset, the moving back drives the ammonia converter in a new limit cycle. This hysteresis pattern (Figure 6) means that the reactor shows one stable limit cycle (the darker line) at the operating pressure of 190 bar, in addition to the static attractors at high conversion (starting point) and to low conversion (cold status); this last one was not reported in Figure 6. Therefore, it could not be possible to obtain the starting conditions by simply inverting the disturbance step on the manipulated variable as performed during the 1988 accident in Germany. However, a slightly higher pressure may change this dynamic pattern. However, at a pressure of 200 bar, the converter goes back to the original steady-state conditions by simply switching back the inlet gas temperature to the starting values. Figure 7 highlights the corresponding different dynamic behaviors at the two distinct pressure values. Similarly, Mancusi et al. (2000) developed a nonlinear analysis for the aforementioned German reactor, and, by selecting the pressure as a bifurcation parameter, they detected two static attractors at the design pressure. In analogy with the results reported here, they also found two static attractors and a limit cycle, but in a different range of the operating pressure (163 bar ÷ 166 bar). Such a different pressure range can be related to a different reactor geometry and size.

In analogy with the approach followed by Morud and Skogestad (1998), a simple linear analysis has been performed to validate the obtained results. In such analysis, the oscillating behavior is explained on the basis of the inverse response and the preheater feedback action. The nonlinear model of the reactor is converted into a linear, state-space, single-input single-output model by means of the pseudo random binary sequence (PRBS) procedure, and the regression algorithm available in the Identification Toolbox of Matlab™. The input and output catalytic bed temperatures are chosen for the identification because of their significance in the thermal recycle effect. Let *G(z)* represent the 1st bed Tin/Tout discrete transfer function, whereas the 2nd bed is neglected because it is not involved in the energy feedback. By defining ϵ as the preheater thermal efficiency, the linear logic scheme is adopted to thermally simulate the 1st bed reactor, and is reported in Figure 8, where it is clearly represented that a greater efficiency means a greater thermal recycle. As seen in Figure 8, it can be stated that

$$t_{out} = t_{in}(1 - \epsilon) + T_{out}\epsilon \tag{6}$$

where t_{in}, t_{out} are the inlet and outlet heat exchanger temperatures of cold-flow side, which is also assumed as the gas with the minor heat capacity. Deriving ϵ from Eq. 6, the following relationship can be deduced

$$\epsilon = \frac{t_{out} - t_{in}}{T_{out} - t_{in}}.$$

If the heat exchanger has a infinite surface, the outlet temperature of the cold side becomes equal to the inlet hot temperature.

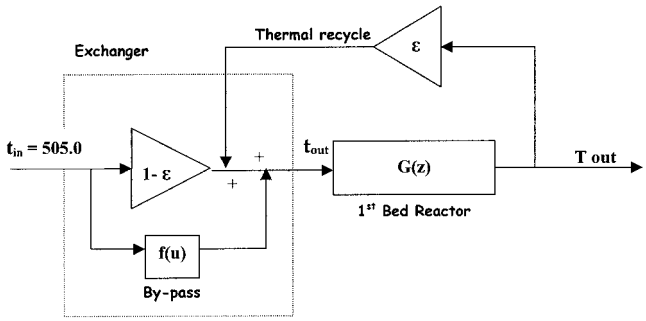

Figure 8. Linear logic scheme adopted to simulate the 1st bed

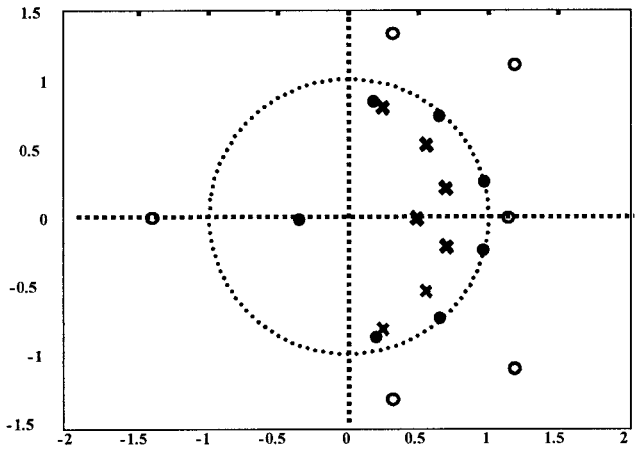

Figure 9. Root locus analysis for the 1st bed plus feed preheater system: x poles at $\epsilon = 0$, ● poles at $\epsilon = 0.54$, ○ zeros.

The presence of inverse response implies zeros outside the circumference of radius one for $G(z)$, whereas an increasing ϵ (that is, feedback effect) moves the poles of the complete system $(G(z)/(1-G(z)\epsilon))$ toward the zeros. The first poles reach the circumference at $\epsilon=0.54$ value deduced by a numerical simulation of the heat exchanger (see Appendix). These are two complex and conjugate poles, and according to the linear system theory, they indicate the presence of instability, which is also in agreement with the existence of a limit cycle solution (see Figure 9).

The Synthesis Loop

The previous paragraph underlines the influence of the preheater on the reactor dynamics, and it shows how the autothermal configuration and the contemporary presence of an inverse time response drives the catalytic reactor conditions to a limit cycle behavior. This section focuses the attention on the overall synthesis loop with the aim of addressing the following specific issues:

- dynamic effect of a more structured heat integration;
- stability impact of heat and material recycles;
- operating conditions range affected by the presence of limit cycles;
- reliable control loop scheme.

The synthesis loop (see Figure 1) is characterized by the presence of two heat recycles adopted to configure the system as much autothermal as possible, and by a material recycle needed to reach the conversion requirements. The recycles increase thermal and material integration, but they also increase sensitivity and structural reliability.

The main model assumptions and philosophy related to the mathematical description of the loops are reported later, whereas more details in terms of model equations are summarized in Appendix A. As previously mentioned, heat exchangers are used to cool down the process stream, leaving the reactor and, thus, separate through condensation, the produced ammonia. Such exchangers are assumed instantaneously at steady-state conditions. Particularly, the models proposed for the three heat exchangers encountered by the process stream, after the reactor, are written without considering the ammonia condensation, because the stream temperature can be always assumed higher than the mixture dew point (in the range of the examined pressures and compositions). In the remaining exchangers, where the ammonia condensation takes place, the RKS equilibrium scheme was adopted to compute the gas and liquid compositions (Reddy and Husain, 1982). Flash drum separators are adopted to separate the liquid ammonia from the recycle stream, and the liquid ammonia from the purge gas. These units, again, are considered instantaneously at stationary condition because the gas phase is the main process phase, which is also interesting, the loop, and, therefore, the corresponding inertial effects (holdups, delay, and so) can be assumed negligible. Data for the calculation of the equilibrium constant were taken from literature (Reid et al., 1988). Purge gas and makeup streams are described by overall mass and energy balances, neglecting the corresponding mixing enthalpy terms.

The most important disturbances having a significant impact on the plant behavior are listed in the following, namely:

- makeup composition;
- makeup temperature;
- variations related to the loop compressor and corresponding disturbances on the loop pressure;
- variations on the liquid ammonia temperature in the last chiller adopted to control the temperature inside the flashing unit.

The first two disturbances can be considered depending on the reforming section. Disturbances on the loop pressure are directly related to the working conditions of the compressor loop. Finally, disturbances on the ammonia temperature can be associated with a bad operation of the refrigeration circuit. Moreover, there are also some minor disturbances, which can act on the synthesis loop, for example, changes in the water and steam flow rates used in the first and in the second heat exchangers, counted from the reactor outlet, which represents the waste heat boiler and boiler feed water preheater, respectively. However, the influence of these last variables is weak if compared with the effect of the aforementioned disturbances. The reason for the greater sensitivity can be found in the phenomena induced by the action of the first listed variations, which directly affect the reactor transient. Any change in composition entering the flash produces a change in the feed composition to the reactor and consequently a different behavior of the unit. A similar effect is determined by a temperature variation of the liquid ammonia in the chiller, and by a change of the loop pressure, which both have a strong impact on the reaction rate. Therefore, in analogy with the accident reported by Morud and Skogestad (1998), the attention here is focused on the effect of pressure disturbances on the loop behavior. Figure 10 shows the temperature transient of the outlet stream from the reactor, when the analyzed system is the reactor alone (case a) or the overall loop (case b). If in the first case it is necessary to reduce the pressure from 195 bar to 185 bar to enter a limit cycle, in the second case, a lower pressure drop down to 190 bar is enough to induce a limit cycle. This confirms the fact that the integrated system behaves in a more sensitive way than the reactor alone.

Similarly, other disturbances previously mentioned can force the same system behavior. However, any actions modifying the feed composition and feed temperature when inducing the limit cycle, generally, are related to a minor step and variation on the

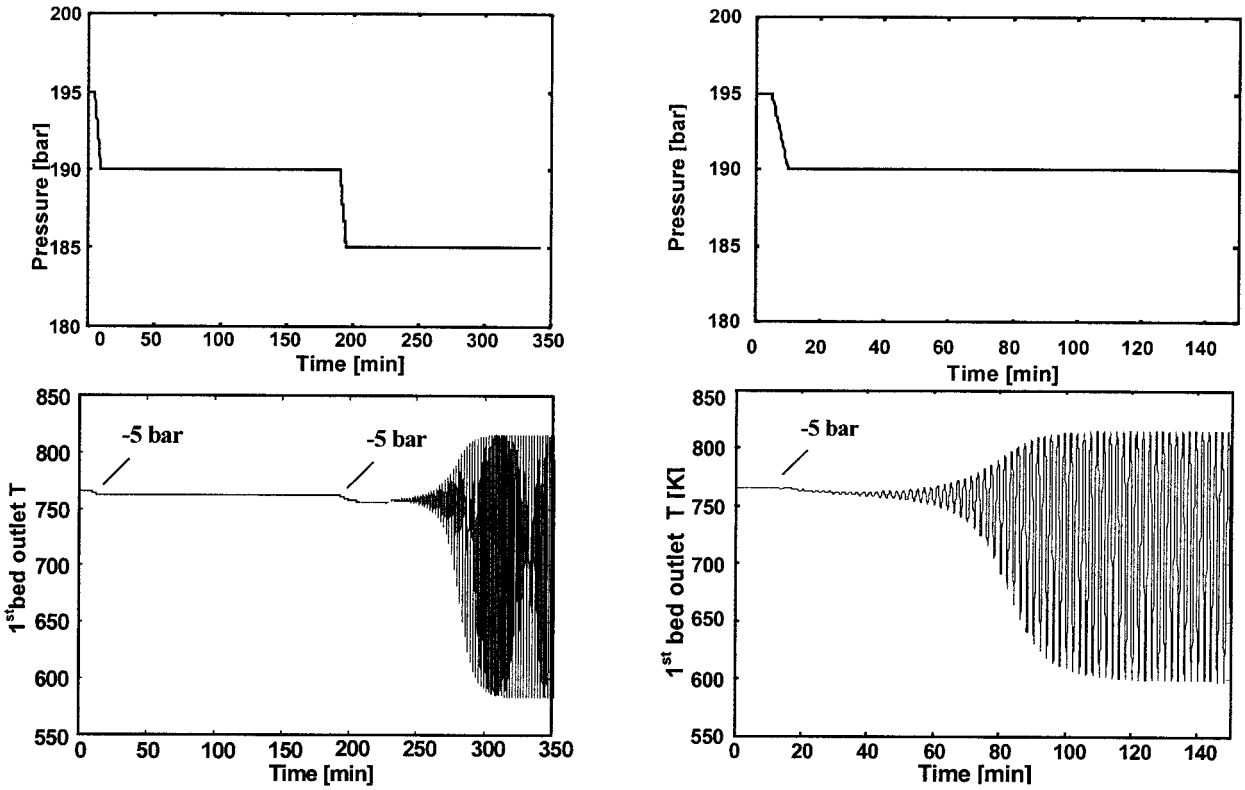

Figure 10. (a) Dynamic behavior of the reactor after two disturbances of 5 bar; (b) dynamic behavior of the overall synthesis loop after a disturbance of 5 bar.

forcing variable, if compared with those adopted for the reactor alone. Mass recycle causes another dangerous effect, slight deviations around the H_2/N_2 optimal ratio and in the makeup stream are amplified in the synthesis loop so that stability and H_2 conversion are threatened. Such a "snowball" effect is clearly shown in Figure 11a where a 1.5% disturbance of the H_2/N_2 ratio in the makeup stream becomes a 17% disturbance of the same ratio in the synthesis loop. Hydrogen conversion starts oscillating in the counter phase with the amount of ammonia recycled to the reactor (see Figure 11b). Here, the reported arrow sketches the path from a stationary condition to a cycle condition characterized by double oscillations of the outlet yield and temperature.

Again, a bifurcation analysis can be more effective in defining ranges and conditions where cycling behavior appears, however, the scope pursued here is underlining the more sensitive system behavior related to the presence of the recycle streams, and, thus, qualitatively confirming the limit cycle conditions for a more restricted pressure variation, or the influence of new variables (that is, H_2/N_2 ratio).

Therefore, because the system becomes more sensitive and, consequently, more potentially dangerous, it is very important to develop a robust and reliable control scheme to reject the disturbances previously mentioned, whereas avoiding the raise of possible oscillating or erratic evolutions.

Control Stratergy for the Synthesis Loop

From the previous analysis, it clearly appears the need for providing a robust control structure for the overall synthesis loop to avoid any possible risks connected with the impact of the aforementioned disturbances. Raising limit cycle behavior or undesired shutdown of the synthesis reactor can involve a consistent damage of the reactor itself, or for the other process units. Sustained oscillations can be dangerous because of the periodic and frequent variations of temperature that can seriously weaken the catalyst.

However, the temperature waves, moving through the heat exchangers cascade, can be amplified up to modifying significantly the loop operating conditions. For example, a reaction temperature change can induce a large variation in the boiler section and in the refrigeration circuit.

In a recent work by Recke et al. (2000) a nonlinear control scheme for the reactor alone has been tested. The results show that hysteresis phenomena can be successfully prevented. Although the oscillation amplitude of the reactor temperature is reduced from 200° C to about 60° C, a limit cycle behavior is still present. In this work, a different approach has been adopted, based on conventional controllers. The main control structure for the synthesis reactor (see Figure 1), and, consequently, for the overall synthesis loop, is based on the exchanger bypass inside the reactor. Here, a fraction of the inlet cold stream is separated from the main flow that cross the heat exchanger, whereas the bypass flow is mixed just before entering the first catalytic bed. The obtained result is a smooth thermal regulation. When the valve is progressively closed, the inlet temperature becomes higher; conversely, by opening the valve, a lower inlet temperature is reached. The most critical condition to be maintained, for safe operations of the reactor, is

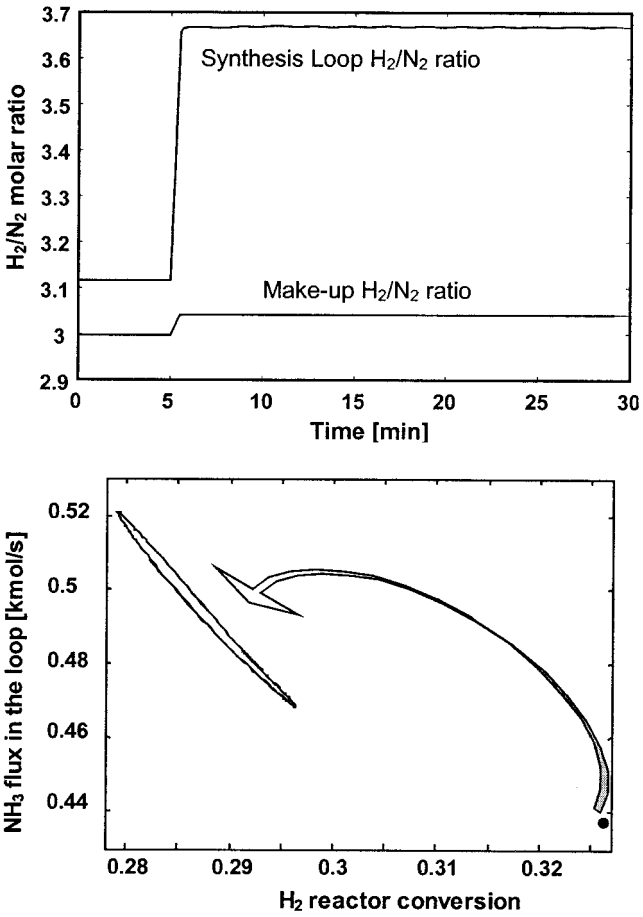

Figure 11. (a) Disturbance of 1.5% on the H_2/N_2 makeup ratio implies a 17% variation on the same ratio inside the synthesis loop. (b) Disturbance of 1.5% on the H_2/N_2 makeup ratio causes a cycle limit behavior.

the inlet temperature of the catalytic bed. Low temperatures may involve the reactor shutdown, whereas high temperatures may lead to a catalyst damage.

From available process data, the correct temperature and flow rate profiles is obtained with a valve position corresponding to a minimum bypass around 1.5% of the total flow. Lower openings cause higher inlet temperatures, whereas higher values lead to the reactor shutdown. As a result, the control system is able to reject all the disturbances that force the valve opening, whereas it is evident that strong disturbances, characterized by a negative action, can easily close completely the valve. This saturated condition leads to an *open loop* system, and, consequently, to the possibility of reaching again a limit cycle behavior, as shown in Figure 12. Therefore, it is necessary to adopt new degrees of freedom to get higher inlet temperatures, and to reject larger disturbances.

For this purpose, we now consider the portion of the loop including the reactor and the first three exchangers (see Figure 1). However, by manipulating the heat duty to the second heat exchanger, the inlet reactor temperature can be significantly modified.

Therefore, it is possible to help the previous controller. The bypass valve of such an exchanger becomes the second manipulated variable, and, in the simulation example examined here, the corresponding valve position of the steady-state condition is around 15% of the valve span. The related controlled variable is the inlet temperature to the second catalytic bed. The reactor inlet temperature does not affect the first bed inlet temperature (until the first controller works), but it modifies the inlet temperature of the second bed through the internal reactor exchanger.

Such behavior of the second controller also justifies the valve position for the inner exchanger bypass (1.5% of the total flow). The former controller is adopted to reduce the inlet temperature (valve opening), whereas the second controller allows the increase of the inlet temperature to be accomplished even if the bypass valve is completely closed.

The same disturbance of -10 bar on the operating pressure may now be rejected by adopting the coupled control configuration (see Figure 13a)

In Figure 13b, a little offset on the higher curve can be noted, representing the 1st bed inlet temperature, which is determined by the 1st completely closed valve. Consequently, the first controller is out of service, but the overall plant is still close to the nominal operating conditions.

Therefore, the two PI temperature control loops adopted have a similar behavior to a split range control configuration. The first one manipulates the inlet temperature to the first bed by reducing the inner thermal recycle; the second loop increases the reactor inlet temperature enhancing the outer thermal recycle.

Two objectives are accomplished by this control configuration:

- Heat saving for the normal operating conditions at both the ammonia loop level and the utilities level (the first and the second exchanger, counted from the reactor outlet, are a steam super heater and a boiler feedwater preheater);
- The second bed inlet temperature is indirectly controlled.

Finally, the sensitivity of the control system has been investigated to single out the most critical parameters. The results show that the proportional gain of the second loop is very critical to reject the aforementioned disturbances. This can be explained by means of the following simple observation: a weak action of the second controller can be compared to the single control loop configuration previously examined. In Figure 14a and 14b, the two controlled, and the two corresponding manipulated variables are, respectively, plotted for a +6 K step disturbance of the ammonia temperature in the last chiller. Here, the gain K_{c1}, computed by the integral tuning method (ISE) is reduced by one order of magnitude. The results show a fast closing of the first valve, and an oscillating action of the

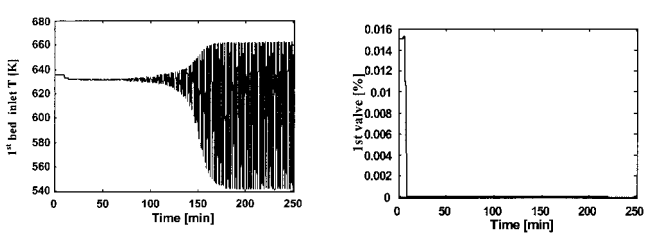

Figure 12. Disturbance of -10 bar forces a total valve closing and it leads to a limit cycle behavior.

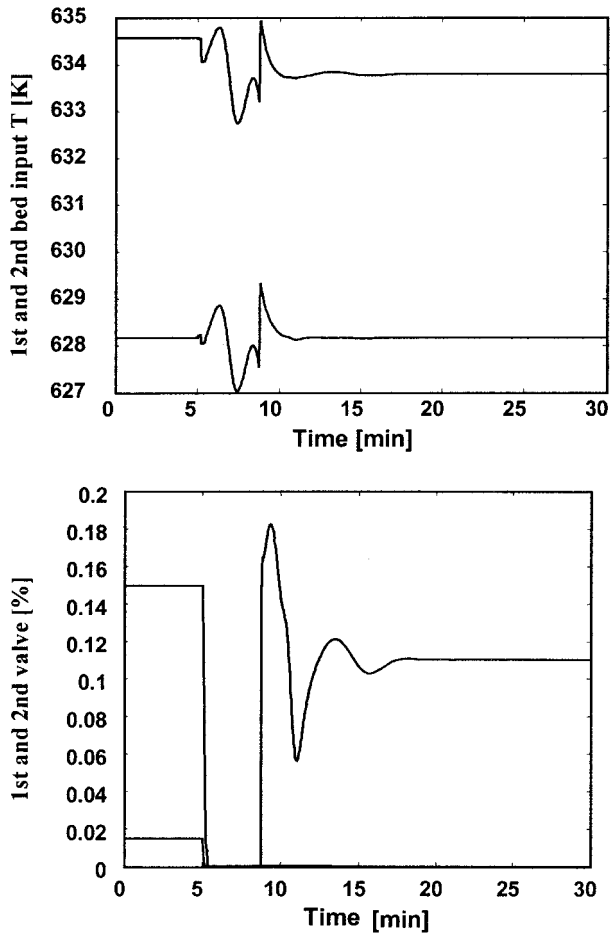

Figure 13. (a) Application of a second control loop avoids the limit cycle (disturbance: 10 bar). (b) 1st valve (darker line) closes completely, but 2nd one stabilizes the system.

second one. The system once again reaches a limit cycle similar to the previous one already shown. A strong positive improvement, in terms of robustness, for this control system, can be achieved by a third control loop, based on the monitoring of the recycle flow rate. Such a control philosophy is well known and discussed in literature, see, for example Luyben and Luyben (1997).

As previously mentioned, Figure 1 shows a complete control scheme. The last loop manipulating the purge valve, which is placed before the syngas makeup, controls the total inlet flow to the reactor. Now, the three manipulated variables of Figure 15a operate very well, and the problems of saturation and oscillation disappear. The disturbance is easily rejected (Figure 15b) even with a disturbance of -10 bars and considering the poor control settings.

With the purpose of stressing the adopted control configuration, and understanding the corresponding behavior with respect to significant pressure variations, some further simulations were carried out imposing a sequence of step increases or step decreases on the reactor pressure. Figure 16a and 16b show the controlled variables and the manipulated ones. The simulation starts from normal operating conditions, and the pressure is increased by 20 bars and then moved back to the initial condition. It can be noted, a total closing of the second valve and the corresponding little offset in the temperature response. A stable behavior is reached and no limit cycle arise.

Moreover, Figure 17a and 17b show the same results in a larger range of pressure variation (−40/+40 bars) and allow the robustness of the designed control configuration to be highlighted and confirmed.

Conclusions

The aforementioned analysis confirmed the results previously reported. Moreover, from the extensive simulations performed, it has been pointed out that the presence of limit cycle behavior and multistability for the ammonia reactor is something independent on the reactor geometry, or the operating conditions, however, it seems to be intrinsically related to the nature of the reaction involved. Such a behavior is strongly dependent on the pressure, and it is also strictly related to the presence of a thermal recycle effect determined by the inlet-outlet exchanger inside the reactor. Moreover, the presence of a main material recycle, because of the unconverted reactants, together with the thermal integration needed for saving energy,

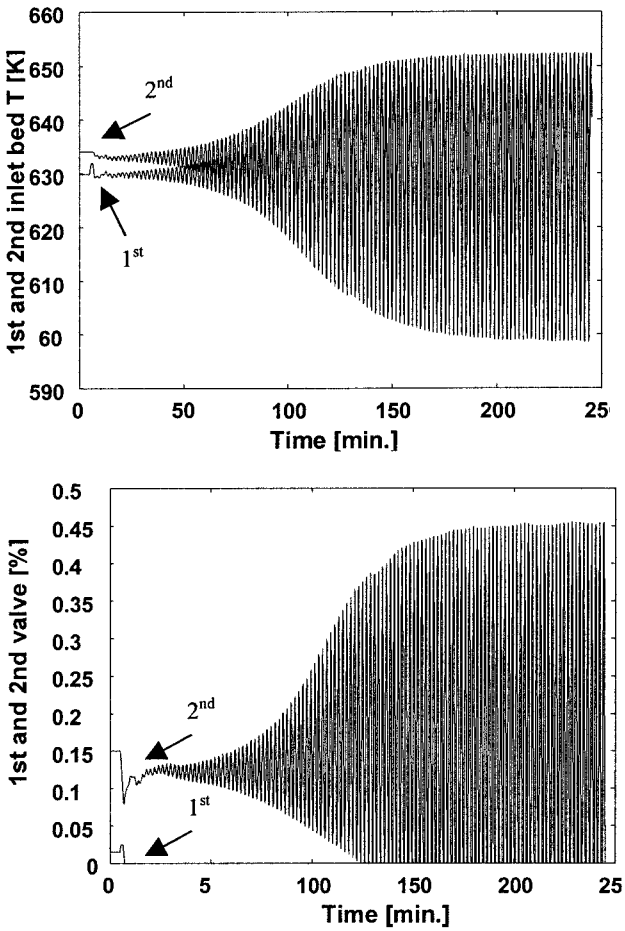

Figure 14. (a) Bad tuning of control parameters leading to a closed loop oscillating behavior (disturbance of +6 K in ammonia cooling system); (b) 1st valve is completely closed, whereas 2nd one starts oscillating.

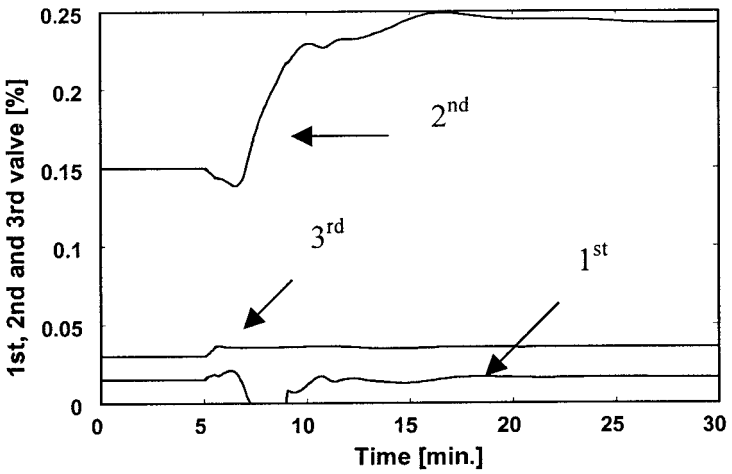

(a)

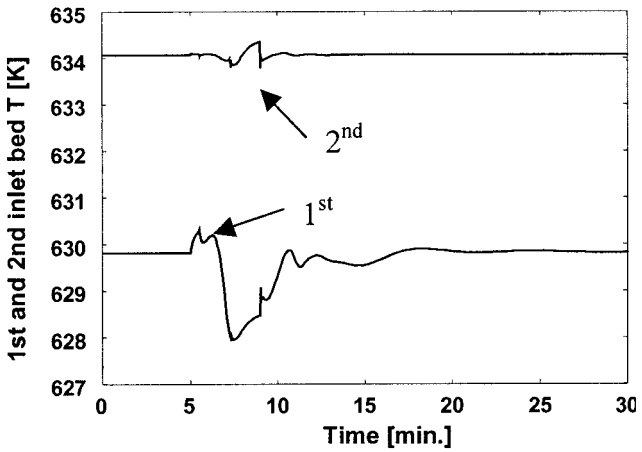

(b)

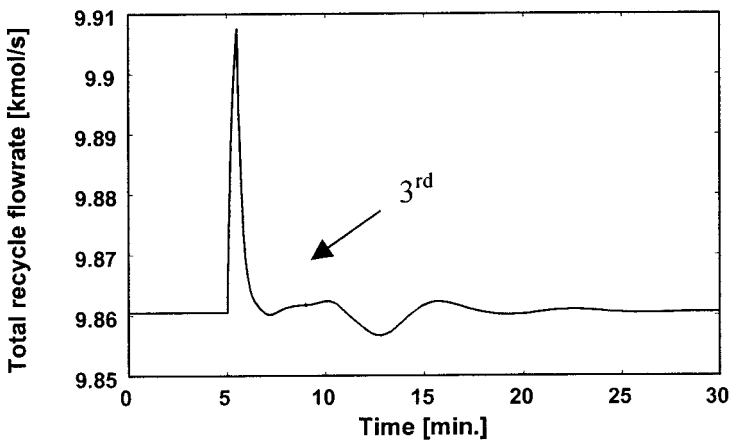

(c)

Figure 15. (a) 1st, 2nd, and 3rd valves [%] opening: the three controllers help the 1st valve to remain partially open; (b) 1st and 2nd controlled temperatures: the set points are reached within 30 min; (c) 3rd controlled variable transient.

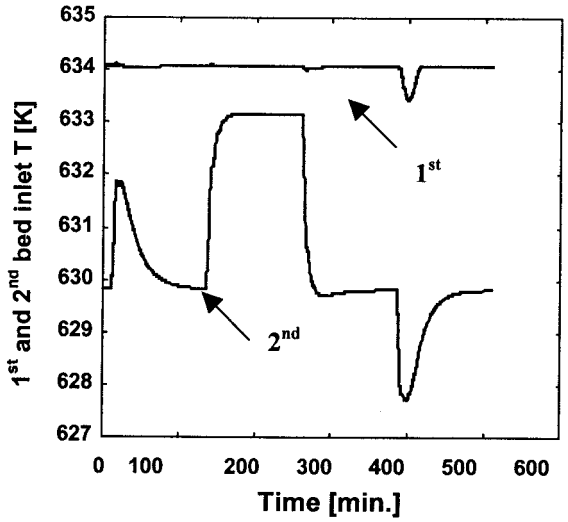

(a)

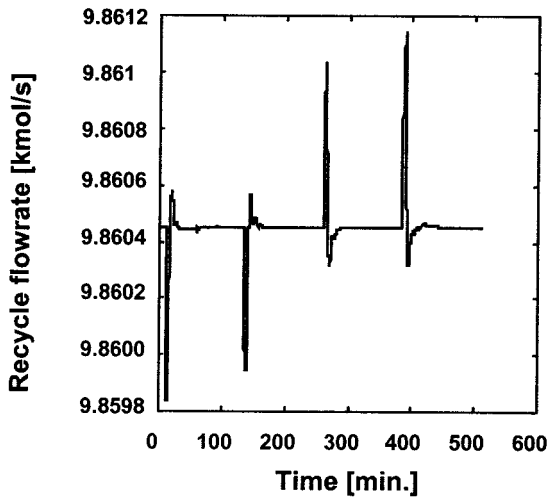

(a)

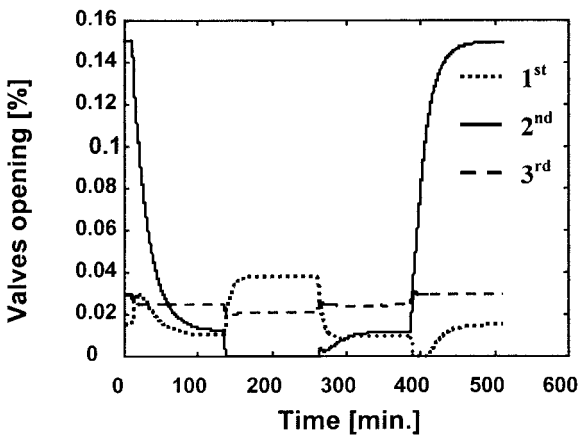

(b)

Figure 16. (a) CVs during a sequence of step disturbances, 2h spaced, on the reactor pressure (10 bar, 10 bar, 10 bar, 10 bar); (b) MVs after a sequence of step disturbances, 2h spaced, on the reactor pressure (10 bar, 10 bar, 10 bar, 10 bar).

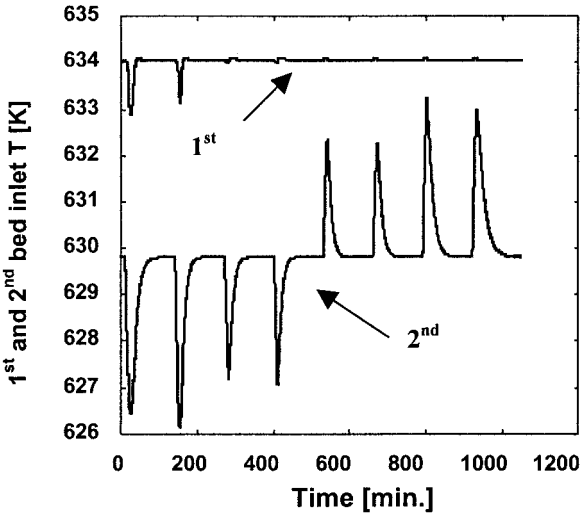

(a)

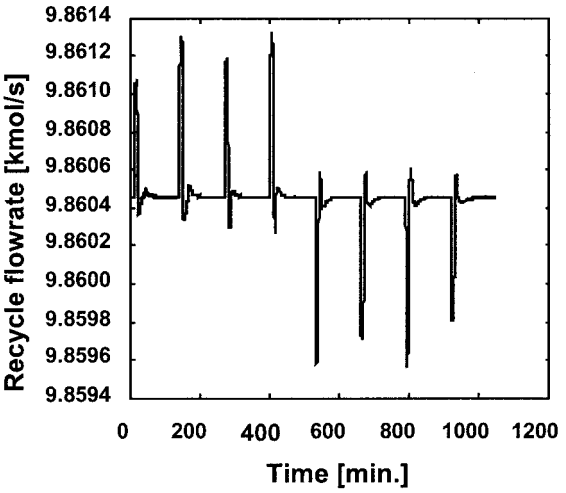

(a)

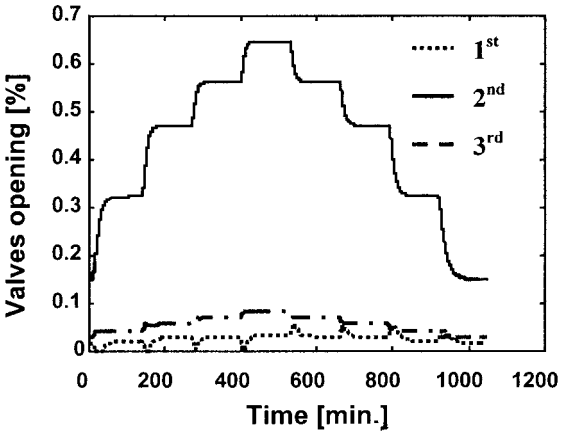

(b)

Figure 17. (a) CVs during a sequence of step disturbances, 2h spaced, on the reactor pressure (-10 bar, -10 bar, -10 bar, -10 bar, 10 bar, 10 bar, 10 bar, 10 bar); (b) MVs after a sequence of step disturbances, 2h spaced, on the reactor pressure (-10 bar, -10 bar, -10 bar, -10 bar, 10 bar, 10bar, 10 bar, 10 bar).

gives rise to a more sensitive plant behavior with limit cycle conditions. Such a limit cycle can be achieved with smaller disturbances compared to the transient of the reactor alone. A snowball effect related to the material recycle completes such a complex paradigm.

In this context it has been shown how a control configuration, based on conventional controllers with:

- the inlet temperature to the first bed reactor;
- the inlet temperature to the second bed reactor;
- the recycle flow rate as controlled variables, and
- the bypass valve across the inlet and outlet internal exchanger
- the bypass valve across the second outlet heat exchanger
- the purge valve of the ammonia chiller

as manipulated variables, gives rise to a reliable process structure able to face the limit cycle behavior in a large range of operating conditions (which means more stability to pressure variations), and in the same time, an increased robustness to a poor tuning of control settings. Values and ranges obtained here are obviously depending on the model, kinetics, parameters and assumptions, however, the scope of this work is to underline the importance of the recycle stream in the context of the possible erratic behavior for the ammonia synthesis loop. The results reported here highlight the reliability of the indicated control structure (even conventional) in reducing system sensitivity to pressure disturbances and poor control settings.

Notation

A = heat exchanger area, m^2
α = specific surface per unit volume, 1/m
α_i = activity of component i
c_i = concentration of component I, kmol/m^3
$C_{p,cat}$ = catalyst specific heat, J/(kg K)
$C_{p,gas}$ = gas specific heat, J/(kg K)
$C_{p,mix}$ = mixture specific heat, J/(kg K)
$D_{i,mix}$ = diffusivity coeff. of component i in the reaction mixture, m^2/s
D_i = internal tubes diameter of the heat exchanger, m
D_e = external tubes diameter of the heat exchanger, m
D_{IN} = internal and external reactor diameter, m
D_{OUT} = external reactor diameter, m
D_S = particle diameter, m
$F_{i,k}$ = gas flow rate of component i from the k^{th} cell, kmol/s
$F_{tot,k}$ = ktotal gas flow rate from the k^{th} cell, kmol/s
g = *of* gravity constant, m/s^2
G_{IN} = specific inlet mass flow rate of the reactor, kg/m^2 s
G_i = internal mass flow rate per unit area, kg/m^2 s
G_e = external mass flow rate per unit area, kg/m^2 s
H = enthalpy flux, W
$\tilde{H}$ = molar enthalpy, J/kmol
h_i = internal heat-transfer coefficient, W/m^2K
h_e = external heat-transfer coefficient, W/m^2K
k = reaction rate constant, 1/h
K_{EQ} = reaction equilibrium constant, $(kmol/m^3)^{-2}$
K_i = liquid-vapor equilibrium constant
k_m = thermal conductivity of metal, W/m K
k_g = thermal conductivity of gas, W/m K
L = liquid flow rate, kmol/s
NC = number of cells for reactor simulation
P = system pressure, Pa
Pr = Prandtl number
Q = heat exchanger duty, W
R_{NH3} = molar rate conversion per unit volume, kmol/(m^3s)
R = gas constant, J/(kmol K)
Re_i = Reynolds number inside tubes
Re_e = Reynolds number outside tubes
Re_{IN} = Reactor inlet Reynolds number
Re_p = particle Reynolds number
T = temperature, K
t = time, s
U = global heat-transfer coefficient, W/(m^2K)
V = vapor flow rate, kmol/s
V_k = volume of the k^{th} cell, m^3
v_O = gas velocity in the empty volume of the bed, m/s
v_x = component x of the gas velocity, m/s
W_c = cold mass flow rate, kg/s
W_h = hot mass flow rate, kg/s
x = radial bed coordinate, m
x_i = liquid molar fraction of component i
y_i = vapor molar fraction of component i
z_i = feed molar fraction of component i

Greek letters

ΔH_{ev} = heat of evaporation, J/kmol
ΔH_r = heat of reaction, J/kmol
$\Delta T_{\ln}$ = mean logarithmic temperature difference, K
ϵ = exchanger thermal efficiency
θ_e = bed void fraction
Ψ = particle-shape coefficient
φ_i = fugacity coefficient for component i
μ = viscosity, kg/(m s)
μ_{mix} = mixture gas viscosity, kg/(m s)
ν_i = stoichiometric coefficient of component i
ρ_{IN} = inlet reactor gas density, kg/m^3
ρ_{OUT} = outlet reactor gas density, kg/m^3
ρ_{gas} = gas density, kg/m^3
ρ_{cat} = catalyst solid density, kg/m^3

Literature Cited

Alessandrini C. G., S. Lynn, and J. M. Prausnitz, "Calculation of Vapor-Liquid Equilibria for the System NH_3-N_2-H_2-Ar-CH_4," *Ind. Eng. Chem.*, **11**, 295 (1972).

Brown P. N., A. C. Hindmarsh, L. R. Petzold, "A Description of DASPK: a Solver for Large Scale Differential-Algebraic System," *Lawrence Livermore National Report*, UCRL (1992).

Dayson D. G., and J. M. Simon, "Kinetic Expression with Diffusion Correction for Ammonia Synthesis on Industrial Catalyst," *Ind. Eng. Chem.*, **7**, 605 (1968).

Froment G. F., K. B. Bischoff, *Chemical Reactor Analysis and Design,* 2nd ed., Wiley, New York (1990).

Gaines D. L., "Ammonia Synthesis Loop Variables Investigated by Steady State Simulation," *Chem. Eng. Sci.*, **34**, 37 (1979).

Kumar A., and P. Dauotidis, "Nonlinear Dynamics and Control of Process System with Recycle," *Proc. of ADCHEM Conf.*, Pisa, Italy (2000).

Jennings J. R., *Catalytic Ammonia Synthesis,* Plenum Press, New York (1991).

Luyben W., and M. Luyben, *Essentials of Process Control,* McGraw Hill, New York (1997).

Mancusi E., G. Merola, S. Crescitelli, and P. L. Maffettone, "Multistability and Hysteresis in an Industrial Ammonia Reactor," *AIChE J.*, **46**, 824 (2000).

Mizsey P., and I. Kalmar, "Effect of Recycle on Control of Chemical Processes," *Comp. Chem. Eng.*, **20**, s883 (1996).

Morud J., and S. Skogestad, "Effect of Recycle on Dynamics and Control of Chemical Processing Plant," *Comp. Chem. Eng.*, **18**, s529 (1994).

Morud J., and S. Skogestad, "The dynamics of Chemical Reactors with Heat Integration, " *Proc. of the European Control Conf.*, Rome, Italy, 2333 (1995).

Morud J., and S. Skogestad, "Analysis of Instability in an Industrial Ammonia Reactor," *AIChE J.*, **44**, 888 (1998).

Nielsen J.B., *Ammonia, Catalysis and Manufacture,* Springer-Verlag, New York (1995).

Pellegrini L., G. Biardi, E. Ranzi, and A. Bacchetta, "Transient Behavior of Catalytic Plug Flow Reactors: The Mixing Cells Model," *La Chimica e L'industria*, **4**, 71 (1988).

Recke B., B. R. Aandersen, and S. B. Jorgensen, "Bifurcation Control of Simple Chemical Reaction Systems," *Proc. of ADCHEM Conf.*, Pisa, Italy, 575 (2000).

Reddy K. V., and A. Husain, "Vapor-Liquid Equilibrium Relationship for

Ammonia in Presence of Other Gases, " *Ind. Eng. Chem.*, **19**, 580 (1980).
Reddy K. V., and A. Husain, "Modeling and Simulation of an Ammonia Synthesis Loop," *Ind. Eng. Chem.*, **21**, 359 (1982).
Reid R. C., J. M. Prausnitz, and B. E. Poling, *The Properties of Gases and Liquids*, Mc Graw Hill, New York (1988).
Stephens A., and R. Richards, "Steady State and Dynamic Analysis of an Ammonia Synthesis Plant," *Automatica*, **9**, 65 (1973).
Ullmann's Encyclopedia of Industrial Chemistry, W. Gerhartz, ed., Weinheim, **A2**, 143, (1985).

Appendix: Basic Model Equations Adopted for the Additional Units

Heat exchanger inside the reactor

The heat exchanger inside the synthesis reactor is a "disk and nuts" exchanger type. The following simple "lump-sum" equations model were adopted to simulate the heat transfer

$$Q = U \cdot A \cdot \Delta T_{\ln} \tag{A1}$$

$$\frac{1}{U} = \frac{1}{h_i} + \frac{D_i}{D_e \cdot h_e} + \frac{D_i \cdot \ln(D_e/D_i)}{2 \cdot k_m} \tag{A2}$$

$$h_i = 0{,}027 \cdot \frac{k_{mix}}{D_i} \cdot \mathrm{Re}_i^{4/5} \cdot \mathrm{Pr}^{1/3} \tag{A3}$$

$$h_e = 0{,}31 \cdot \frac{k_{mix}}{D_e} \cdot \mathrm{Re}_e^{0.554} \cdot \mathrm{Pr}^{1/3} \tag{A4}$$

where

$$\mathrm{Re}_e = \frac{D_e \cdot G_e}{\mu_m} \qquad \mathrm{Re}_i = \frac{D_i \cdot G_i}{\mu_m} \qquad \mathrm{Pr} = \frac{\mu \cdot c_p}{k_{mix}}$$

Kinetic expression for the reaction rate

The kinetic relationship adopted is a Temkin and Pyzev modified equation. As proposed by Dayson and Simon (1968), instead of the simple partial pressure for each component, the fugacity correction has been used

$$R_{NH_3} = 2k \cdot \left(K_{EQ}^2 \cdot a_{N_2} \cdot \left[\frac{a_{H_2}^3}{a_{NH_3}^2} \right]^{\alpha} - \left[\frac{a_{NH_3}^2}{a_{H_2}^3} \right]^{1-\alpha} \right) \tag{A5}$$

where the multiplying factor $2k$ is evaluated from

$$2k = 1.7698 \times 10^{15} \cdot \exp\left(-\frac{40765}{RT} \right) \tag{A6}$$

and the equilibrium constant is calculated with

$$Log_{10} K_{EQ} = -2.691122 \cdot Log_{10} T - 5.519265 \times 10^{-5} \cdot T + 1.848863 \times 10^{-7} \cdot T^2 + \frac{2001.6}{T} + 2.6899 \tag{A7}$$

Expression for the fugacity coefficients are the following ones (Dayson and Simon, 1968)

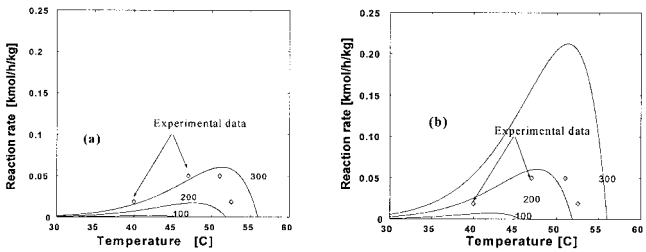

Figure A1. Reaction rate vs. temperature, at different operating pressures: (a) the reaction rate without correcting factor; (b) the reaction rate is multiplied by 3.5.

$$\varphi_{H_2} = \exp(P \cdot \exp(-3.8402 \cdot (T^{0.125}) + 0.541) - (P^2 \cdot \exp(-0.1263 \cdot T^{0.5} - 15980) + 300 \cdot \exp(-0.011901 \cdot T - 5.941) \cdot (\exp(-P/300) - 1)) \tag{A8}$$

$$\varphi_{N_2} = 0.93431737 + 0.3101804 \times 10^{-3} \cdot T + 0.295896 \times P - 0.2707279 \times 10^{-6} \cdot T^2 + 0.47750207 \times 10^{-6} \cdot P^2 \tag{A9}$$

$$\varphi_{NH_3} = 0.1438996 + 0.202538 \times 10^{-2} \cdot T + 0.4487672 \times 10^{-3} \cdot P - 0.1142945 \times 10^{-5} \cdot T^2 + 0.2761216 \times 10^{-6} \cdot P^2 \tag{A10}$$

In Figure 1a a comparison is reported between calculated curves and experimental data taken from the literature (Ullmann's, 1985). To match these data, it was necessary to multiply the reaction rate by a factor $f = 3.50$. This coefficient, as underlined by Morud and Skogestad (1998), takes into account the higher activity of the new generation of catalysts. The lower value of factor f, compared with that suggested by Morud and Skogestad (1998), can be explained by the more accurate expression adopted for the reaction rate (Eq. A5).

Heat exchangers models in the Synthesis loop

Simple steady-state equations are adopted for the first heat exchanger, where the water is evaporated to produce high-pressure steam

$$Q = U \cdot A \cdot \Delta T_{\ln} \tag{A11}$$

$$Cp_{mix,h} \cdot W_h \cdot (T_{in,h} - T_{out,h}) - Q = 0 \tag{A12}$$

$$W_{H_2O} \cdot \Delta H_{ev}(T_{H_2O}) - Q = 0 \tag{A13}$$

The second and the third gas-gas exchangers are described by the following equations

$$Q = U \cdot A \cdot \Delta T_{\ln} \tag{A14}$$

$$Cp_{mix,c} \cdot W_c \cdot (T_{in,c} - T_{out,c}) - Q = 0 \tag{A15}$$

$$Cp_{mix,h} \cdot W_h \cdot (T_{in,h} - T_{out,h}) - Q = 0 \tag{A16}$$

where all the $U \cdot A$ terms have been assumed constant in the analyzed range of the process conditions.

To evaluate the hot stream outlet temperature, where the ammonia condensation takes place, a global approach is adopted through RKS equilibrium calculation performed at the inlet and outlet condition of the exchanger

$$W_{NH_3} \cdot \Delta H_{ev,NH_3}(T_{NH_3}) - Q = 0 \tag{A17}$$

$$\dot{H}_{tot,h}(T^{IN}) - \dot{H}_{tot,h}(T^{OUT}) - Q = 0 \tag{A18}$$

$$F \cdot z_i - L \cdot x_i - V \cdot y_i = 0 \tag{A19}$$

$$y_i = K_i \cdot x_i \tag{A20}$$

$$K_i = K_i(T^{OUT}, P, x_i, y_i) \tag{A21}$$

$$Q = U \cdot S \cdot \Delta T_{\ln}(T_{NH_3}, T_h^{IN}, T_h^{OUT}) \tag{A22}$$

$$H^{gas}(T) = Cp^{gas} \cdot (T - T_{RIF}) \tag{A23}$$

$$\dot{H}_{tot,h}(T) = W_{NH_3}^{l} \cdot H_{NH_3}^{l}(T) + W_{mix}^{gas} \cdot H_{mix}^{gas}(T) \tag{A24}$$

$$H^{liq}(T) = Cp^{liq} \cdot (T - T_{RIF}) - \Delta H_{ev,NH_3}(T_{RIF}) \tag{A25}$$

Flash drum model

Finally, thermodynamic data used in the flash simulation are derived from Reid et al. (1988) and the equations adopted for the flash, with the hypothesis of adiabatic and isobaric conditions, are simply given as

$$F \cdot \tilde{H}_F - L \cdot \tilde{H}_L - V \cdot \tilde{H}_V = 0 \tag{A26}$$

$$F \cdot z_i - L \cdot x_i - V \cdot y_i = 0 \tag{A27}$$

$$y_i = K_i \cdot x_i \tag{A28}$$

$$K_i = K_i(T, P, x_i, y_i) \tag{A29}$$

$$\tilde{H}_L = \tilde{H}_L(T, x_i) \tag{A30}$$

$$\tilde{H}_V = \tilde{H}_V(T, y_i) \tag{A31}$$

$$\tilde{H}_F = \tilde{H}_F(T_F, z_i) \tag{A32}$$

Manuscript received Dec. 27, 2001, revision received Sept. 8, 2003, and final revision received Jan. 12, 2004.